Title: Frequency-specific hemispheric bias in phase entrainment of neural oscillations in unilateral spatial neglect

Abbreviated title: Hemispheric entrainment bias in USN

Yuka O. Okazaki[1, 2, *], Noriaki Hattori[3], Teiji Kawano[4], Megumi Hatakenaka[4], Ichiro Miyai[4], and Keiichi Kitajo[1, 2, 5*]

1. Division of Neural Dynamics, Department of System Neuroscience, National Institute for Physiological Sciences, National Institutes of Natural Sciences, Okazaki, Aichi, 444-8585, Japan
2. Physiological Sciences Program, Department of Advanced Studies, Graduate Institute for Advanced Studies, Graduate University for Advanced Studies (SOKENDAI), Okazaki, Aichi, 444-8585, Japan
3. Department of Rehabilitation, University of Toyama 930-0194, Japan
4. Neurorehabilitation Research Institute, Morinomiya Hospital, Osaka, 536-0025, Japan
5. RIKEN CBS-TOYOTA Collaboration Center, RIKEN Center for Brain Science, Wako, 351-0198, Japan

*Corresponding authors: Yuka O. Okazaki, yokazaki@nips.ac.jp; Keiichi Kitajo, kkitajo@nips.ac.jp

Number of pages: 31

Number of tables: 1 and number of figures: 8

Number of words for abstract: 250 introduction: 650, and discussion: 1442

Conflict of interest

The authors declare no competing financial interests

Acknowledgments

This work was supported in part by the NINS OPEN MIX LAB Program (NINS Program No. OML032401); a research grant from TOYOTA Motor Corporation to KK; and a grant-in-aid for General Research on Adult Diseases Including Cardiovascular Diseases and Diabetes (23FA1015) from the Japanese Ministry of Health, Labor and Welfare to IM. We also thank Dr. Hroshi Yokoyama for providing the code for the transfer entropy analysis.

Abstract

Left unilateral spatial neglect (USN), typically caused by a right hemisphere lesion, impairs left-side stimulus perception. Attention influences perception via cortical oscillations, shown as phase shifts and power changes in electroencephalography (EEG). Given this relationship, USN may stem from hemispheric imbalance in synchronizing cortical oscillations internally and externally. We studied this using steady-state visual evoked potentials (SSVEPs) from flickering stimuli of various frequencies. Our study included USN and non-USN patients with a right hemisphere lesion, but no hemianopsia, as well as healthy controls. Importantly, we confirmed that the affected hemisphere's visual cortex in both patient groups responded to all flickering frequencies, ensuring a valid comparison. Comparing SSVEP power between the intact and affected hemispheres revealed no differences in non-USN patients. In USN patients, both hemispheres responded equally to most frequencies; however, SSVEP power was enhanced in the intact visual cortex with 9-Hz stimulation, resulting in a significant hemispheric bias. This bias was not caused by deficiencies in generating oscillations (we observed no significant differences in spontaneous pre-stimulus alpha oscillations) but rather by abnormal alpha-band synchronization with external inputs. Further analyses revealed increased phase-amplitude coupling between alpha phase and gamma amplitude in the intact hemisphere and elevated transfer entropy from the right visual cortex to the left frontal cortex in USN patients. These results reveal that USN involves complex alterations in neural synchronization stemming from imbalanced entrainment of oscillators to alpha-frequency stimuli, beyond merely local damage. This alpha-specific effect provides insights into frequency-specific synchronization in spatial attention, potentially guiding targeted therapies.

Significance Statement

This study provides crucial insight into the neural mechanisms underlying unilateral spatial neglect (USN), a sequela of stroke. By examining the frequency-specific hemispheric bias in neural synchronization, we identified a significant imbalance in brain activity, particularly in the alpha frequency range. This imbalance was not merely a result of local deficits but involved complex compensatory mechanisms at both the local and global network levels. Our findings highlight how disrupted neural oscillations and impairments in the capacity to modulate these oscillations for synchronization contribute to cognitive deficits in patients with USN. This research addresses gaps in our understanding of attention function and disorders, which will aid the development of more targeted therapeutic interventions and rehabilitation strategies.

Introduction

Left unilateral spatial neglect (USN) is a neurological disorder characterized by an inability to notice objects on the left side despite having no visual field deficits. This condition is associated with impairment of the right dorsal attention network, particularly in the right parietal lobe (Mort et al., 2003; Corbetta et al., 2005), and the superior temporal gyrus (Karnath, 2001; Karnath et al., 2001). Furthermore, the occipital and frontal white matter tracts are also typically affected (Thiebaut de Schotten et al., 2005). The dorsal attention network (Corbetta and Shulman, 2002), including the frontal eye fields and bilateral parietal sulci, has spatial maps representing contralateral space. The attentional functions associated with these spatial maps in the left and right hemispheres are balanced via reciprocal inhibitory interactions (Grefkes and Fink, 2011). Disruption of this network leads to hyperactivity of the structurally intact left hemispheric circuits, which influences bottom-up sensory responses and causes a rightward bias in attention and perception (Corbetta et al., 2005; He et al., 2007). Thus, USN arises from a disruption of hemispheric balance in the attentional networks.

The capacity to modulate neural oscillations is critical for attentional focus. Indeed, recent studies have indicated that during sustained attention, perceptual sensitivity fluctuates periodically, which suggests periodic sampling of the visual environment (Fiebelkorn et al., 2013; Fiebelkorn et al., 2018). These attentional fluctuations are related to the phase of spontaneous neural oscillations, which reflect cortical excitability and influence perception. In the visual cortex, alpha oscillation phases predict visual stimulus detection performance (Busch et al., 2009; Mathewson et al., 2009). When stimuli are rhythmically and predictably presented, visual target detection is most sensitive at a specific timing synchronized with this rhythm (Mathewson et al., 2010). This synchronization is due to the alignment of high excitatory phases of oscillations, under strong top-down control (Lakatos et al., 2008; Schroeder and Lakatos, 2009; Besle et al., 2011). These findings suggest that attentional systems control not only spatial location but also the timing of attentional focus via the synchronization of neural oscillations. Therefore, abnormalities in the capacity to modulate these oscillations may be a critical contributing factor to the attentional deficits observed in patients with USN. However, this has not been specifically investigated.

Impaired neural synchrony is evident in disorders such as schizophrenia and autism, as measured via steady-state evoked responses (SSERs) to repetitive sensory stimuli. In patients with schizophrenia (Kwon

et al., 1999; Krishnan et al., 2005) and autism (Wilson et al., 2007; Rojas et al., 2011), SSERs, which involve frequency- and phase-synchronized neural responses, show a selective reduction in gamma oscillations in response to visual or auditory stimuli of different frequencies. SSERs appear as an increase in amplitude due to the periodic alignment of the spontaneous oscillation phase at the stimulus frequency; this is known as entrainment (Notbohm et al., 2016). Entrainment is most effective when the stimulation frequency is close to the system's natural frequency (Pikovsky et al., 2003; Okazaki et al., 2021). This suggests that a power reduction, limited to gamma oscillations in these diseases, is due to impairment in the underlying system responsible for gamma oscillations. Thus, a steady-state paradigm is ideal for probing the capacity of neural networks to generate and synchronize oscillatory activity in specific frequency bands with a high signal-noise ratio.

In the present study, we measured SSERs to visual stimuli of different frequencies in the USN and control groups (stroke patients without USN and healthy participants) to examine abnormalities in the synchronization system. Neither patient group was accompanied by hemianopsia, and local bottom-up responses in the visual cortex of the lesioned hemisphere should not be significantly impaired. However, the entrainment of ongoing oscillations driven by a network generating oscillations at a specific frequency can be diminished. If attention coordinates excitation and inhibition with the timing of external stimuli, we would expect patients with USN to exhibit a hemispheric imbalance in the specific frequency of the response to periodic stimuli.

Materials and Methods

Participants

The study consisted of three groups: USN patients (n = 21), stroke patients without USN (n = 38), and healthy control participants (n = 17). We recruited patients who had been admitted to the Kaifukuki (Convalescent) Rehabilitation Ward of Morinomiya Hospital. The inclusion criteria for stroke patients were: (1) first-episode stroke, (2) right hemisphere cortical/subcortical lesion without hemianopsia, (3) cerebral infarction, and (4) male. For healthy participants, the inclusion criteria were: (1) no history of stroke, (2) full scores on all neuropsychological assessments, and (3) male to match the patient group. All participants provided written informed consent. The study was approved by the Institutional Review Boards of RIKEN, the National Institutes of Natural Sciences, and Morinomiya Hospital.

Clinical assessment of stroke

Electroencephalography (EEG) measurements and clinical assessments were performed by trained investigators approximately 1 month after stroke onset. The diagnosis of USN was comprehensively determined by the attending physician based on regular clinical examinations, including the Behavioural Inattention Test (BIT). Motor impairment was assessed using the Fugl-Meyer Assessment upper extremity (FMA-UE) and lower extremity (FMA-LE), and activities of daily living were assessed using the Functional Independence Measure motor (FIM-M) and cognitive (FIM-C) scores. For all scales, a lower score indicates greater disability. To match the severity of the USN and non-USN groups, we selected 21 non-USN patients in ascending order of the Mahalanobis square distance, d_i^2, to the USN patient within a four-dimensional space of the clinical score:

$$d_i = \sqrt{(\boldsymbol{y}_i - \boldsymbol{\mu})\,\Sigma^{-1}(\boldsymbol{y}_i - \boldsymbol{\mu})^T},$$

where $\boldsymbol{y}_i$ is the i-th non-USN patient's clinical scores and $\boldsymbol{\mu}$ and Σ are the mean and covariance matrix of the USN samples, respectively. The demographic information and clinical scores of each group are listed in Table 1. An unpaired t-test confirmed that there were no significant differences between the groups in any of the scores.

Experimental Design

EEG was recorded from 19 Ag/AgCl electrodes in the 10-20 system configuration using a NeuroFax EEG 1224 system (Nihon Kohden, Tokyo, Japan; sampling rate: 500 Hz; bandpass filter: 0.53–120 Hz; ground electrode: forehead; reference: left earlobe). Under an eyes-closed resting condition, a strobe light flickered at frequencies ranging from 3 to 30 Hz in 3-Hz steps. Each frequency flicker stimulus was presented for 10 s with a 10-s interval (Figure 1).

Preprocessing

The EEG signals were first re-referenced offline to the average of the right and left earlobe signals. We applied wavelet-enhanced independent component analysis (wICA) to eliminate intermittent high-amplitude artifacts (Castellanos and Makarov, 2006). This method decomposes the EEG signals into independent

components (ICs), and a discrete wavelet transform is applied to each IC. Wavelet coefficients defined as artifacts based on the level-dependent threshold of the wavelet decomposition are zeroed, and artifact-free ICs are extracted from the inverse wavelet transform on this result. Thus, the entire IC, which contains a significant amount of neural signals, need not be excluded, as in the case of conventional ICA denoising.

Steady-state visual evoked potential (SSVEP)

To evaluate the neural response during the flickering stimulation, the frequency power spectrum for each stimulus condition was obtained using the Fourier transform (Hanning window, frequency range: 1–35 Hz). The Fourier transform was applied to the data with a 1-s window during the 10-s flicker interval and averaged for each stimulus frequency condition.

Phase-amplitude coupling (PAC)

We evaluated PAC using the modulation index (MI) (Tort et al., 2010) to determine how high-frequency oscillations are co-modulated by a low-frequency phase when neural oscillations are entrained to rhythmic external stimuli. Instantaneous phase and amplitude were extracted via wavelet transform at the center frequency, f, and time, t, with the standard deviation (SD), $\sigma f = 4f/m$, $\sigma t = m/2\pi f$, and constant, m, set to 4 (Lachaux et al., 2000). We focused on the PAC between the alpha (6–12 Hz) phase and the gamma (30–55 Hz) amplitude for 10 s during the 9-Hz flickering stimulus.

To derive the MI for each frequency pair of α phase and γ amplitude, the given α frequency phase was divided into 20 bins, and the mean γ amplitude in each bin was calculated. This provided a phase-amplitude distribution for each frequency pair, and the MI was obtained according to the Kullback-Leibler divergence between the observed distribution and the circular uniform distribution. An MI of 0 indicates that the amplitudes are the same for all phase bins (i.e., a circular uniform distribution) and that there is zero PAC, whereas an MI of 1 indicates maximum coupling.

Transfer entropy (TE)

To quantitatively investigate the direction and strength of information transfer between brain regions in response to flickering stimuli, we performed TE analysis (Schreiber, 2000). After applying an 8.5–9.5 Hz FIR bandpass filter to the EEG responses to 9-Hz flickering stimuli, we extracted the amplitude from the

analytic signal using the Hilbert transform. TE was calculated for all pairs of electrodes for these amplitude data during the flickering stimulus interval. To estimate the probability distributions required for TE calculation, we generated histograms for the amplitude data, with bin sizes according to Sturges' rule (Legg et al., 2013). $TE_{Y\rightarrow X}$ quantifies the extent to which knowledge of the state of system *Y* at time *t* contributes to predicting the one-step future state of system *X* at time $t+\tau$, beyond the predictability provided by the state of *X* at time *t* alone. The formula for TE is given by:

$$TE_{Y\rightarrow X(\tau)} = \sum p(x_{t+\tau}, x_t, y_t) \log_2 \frac{p(x_{t+\tau}|x_t, y_t)}{p(x_{t+\tau}|x_t)},$$

where $p(x_{t+\tau}, x_t, y_t)$ denotes the joint probability of observing the future state of *X* at time $t+\tau$ along with the states of *X* and *Y* at time *t*. Here, *x* and *y* represent the observed data derived from the systems *X* and *Y*, respectively. The terms $p(x_{t+\tau}|x_t, y_t)$ and $p(x_{t+\tau}|x_t)$ denote the conditional probabilities of the one-step future state of *X*, given its state at time *t* with and without considering the state of *Y* at time *t*.

In this analysis, amplitude data from the first 0.5 s of the flickering stimulus interval were used as past observations, x_t, y_t, and amplitude data from one sample ahead in time were used as future observations, $x_{t+\tau}$. TE was calculated by varying the delay, τ, from 0 to 5 s in 0.1-s steps. The optimal delay, δ, was determined by maximizing *TE* with respect to τ:

$$\delta = \arg\max_u \left(TE_{Y\rightarrow X(\tau)}\right).$$

Statistical analysis

To statistically test for differences in SSVEP between the left and right hemispheres, we used a linear mixed model with hemisphere (left and right), flicker frequency (3, 6, 9, 12, 15, 18, 21, 24, 27, and 30 Hz), and group (USN patients, non-USN patients, and healthy controls) as fixed factors and subjects as random factors, with the exclusion of outliers 1.5 times over the interquartile range.

To statistically test for differences in PAC between the left and right hemispheres, we performed a cluster-based permutation test (Maris and Oostenveld, 2007). The MI was calculated for each permutation dataset generated by random reassignment of O1 and O2 electrode labels. For each permutation, clusters were identified from adjacent data points showing statistically significant hemispheric differences in MI, and the sum of the *t*-values within these clusters was determined as a cluster-level statistic. Only the largest value of

the cluster-level statistic obtained for each permutation was selected, and this procedure was repeated 1000 times to construct the distribution of the cluster-level statistic under the null hypothesis. A cluster of hemispheric differences in the original data was considered statistically significant if it exceeded the 95th percentile of this distribution.

Results

SSVEP power in the affected hemisphere

We included only stroke patients without hemianopsia. Therefore, to confirm that the visual cortex of the affected (right) hemisphere could respond to visual stimuli, we plotted SSVEP power at the O2 electrode as a function of the flicker and response frequencies (Figure 2). When compared with the power spectrum of the baseline period, a clear fundamental can be seen on the diagonal (black dashed line), which indicates that the visual cortex of the affected hemisphere was precisely enhanced at the flicker frequency.

Hemispheric imbalance of the SSVEP

The SSVEP power of the affected (right) hemisphere (O2 electrode) was compared with that of the intact (left) hemisphere (O1 electrode) to investigate hemispheric balance in frequency responses. We found a significant hemisphere × flicker frequency × group interaction ($F = 2.09$, $p < 0.005$). To further investigate this interaction, simple main effects test were conducted for hemisphere differences at each frequency within each group, with a Bonferroni correction applied for multiple comparisons. Within the USN group, SSVEP power of the intact hemisphere was significantly greater than that of the affected hemisphere at 9 Hz ($F = 62.36$, $p < 0.001$). No significant hemisphere differences were observed at other frequencies within the USN group. In the non-USN and healthy control groups, there were no significant hemisphere differences at any frequency after Bonferroni correction. Figure 3 shows the hemispheric difference in SSVEP power (O1 - O2) corresponding to stimulation frequency. This suggests that frequency-specific hemispheric bias is the factor that separates USN from non-USN patients.

We applied the same analysis for the central (C3, C4) and frontal (F3, F4) electrodes to verify the frequency response of hemispheric bias outside the visual area. Figure 4 shows the difference in SSVEPs between C3 and C4 electrodes (upper panels) and between F3 and F4 electrodes (lower panels) at each frequency. We found no significant main effects for hemisphere or interactions in either the central or frontal

regions.

Hyperactivity of the intact hemisphere

To determine whether the hemispheric imbalance of SSVEP power confined to 9 Hz in the USN group was attributed to the intact (left) or affected (right) hemisphere, we compared SSVEP power at 9 Hz in the corresponding hemisphere in the healthy controls (Figure 5, left panel). A simple main effects test showed a significant effect of group on SSVEP power in the left hemisphere ($F = 6.66$, $p < 0.005$) and in the right hemisphere ($F = 10.58$, $p < 0.001$). Post-hoc comparisons with Bonferroni correction indicated that in the left hemisphere, both the USN and the non-USN group had significantly higher SSVEP power than the healthy control group ($p < 0.005$ and $p < 0.05$, respectively). In the right hemisphere, the non-USN group showed significantly higher SSVEP power than the healthy control group ($p < 0.005$), while the USN group did not differ significantly from the healthy controls. We also examined the resting state interval (i.e., before the photo flicker session) and found no significant differences in either the USN or non-USN group (Figure 5, right panel). Taken together, there was no major abnormality in the spontaneous generation of alpha oscillations in the USN group; rather, it was the capacity to synchronize these oscillations with other external oscillations that differed between the hemispheres in the USN group.

Hemispheric imbalance of PAC

We investigated PAC given that higher frequency oscillations may be cooperatively modulated when neural oscillations are entrained by rhythmic external stimuli. PAC was assessed using the MI for 9-Hz flickering stimuli (Figure 6). We hypothesized that the intact left hemisphere, which showed enhanced SSVEP, would exhibit stronger PAC. Thus, we performed a cluster-based permutation test to examine hemispheric differences. Results showed a significant hemispheric bias in PAC between the alpha (7–12 Hz) phase and gamma (35–45 Hz) amplitude in the USN group. Specifically, the MI was higher in the intact hemisphere than in the affected hemisphere ($p < 0.05$, one-tailed) peaking at the 9-Hz phase. These effects were not observed in the non-USN or healthy control group. This suggests that gamma activity is modulated by the alpha phase aligned to the 9-Hz flicker stimulation and that this modulation is particularly enhanced in the intact hemisphere of the USN group.

Hemispheric imbalance of TE

In USN and non-USN patients with right hemisphere damage, we aimed to clarify how information is transferred from the responsive visual cortex to other brain regions. Here, we used TE to examine the pattern of information transfer from the O1 and O2 electrodes to the left and right frontal electrodes (Figure 7). Results showed that in the USN group, there was significantly greater information flow from the right visual area (O2 electrode) than from the left visual area (O1 electrode) to the intact left frontal areas ($t = -2.7$, $p < 0.05$, paired *t*-test). This enhancement was significantly greater than that in the healthy control group ($t = -2.89$, $p < 0.01$, unpaired *t*-test; Figure 7, left panel in the feedforward direction). This indicates a hemispheric bias in information transfer in the feedforward direction in USN patients. In contrast, no such bias was observed in non-USN patients ($t = -0.47$, $p = 0.64$, paired *t*-test) or healthy controls ($t = 1.42$, $p = 0.174$, paired *t*-test). In addition, there were no significant differences in information flow from the O1/O2 electrodes to the affected right frontal areas (Fig. 7, right panel in the feedforward direction) or in the feedback direction (i.e., from the left/right frontal areas to the O1/O2 electrodes) in any group (Figure 7, lower panels). These findings suggest that the distinct clinical symptoms of USN are not solely due to biased local brain activity but are closely related to asymmetric information transfer, especially in the feedforward direction.

Correlation between SSVEP power and USN severity

To investigate the relationship between neural synchronization capacity and symptom severity in USN patients, we performed Pearson's correlation analysis between SSVEP power and BIT scores. Results showed a significant positive correlation between SSVEP power at 9 Hz in the right hemisphere (O2 electrode) and BIT score (Pearson's $r = 0.70$, $p < 0.01$). That is, the higher the SSVEP power at 9 Hz in the right hemisphere, the milder the USN symptoms. In contrast, there was no significant correlation in the left hemisphere (O1 electrode; Pearson's $r = 0.38$, $p = 0.18$; Figure 8, upper panels). Additionally, to examine the frequency-specific nature of the relationship between SSVEP power and USN severity, we analyzed correlations across all stimulation frequencies. Significant correlations between SSVEP power and BIT score were observed only at 9 and 12 Hz in the right hemisphere (Pearson's $r = 0.70$, $p < 0.01$, for both frequencies, FDR-corrected; Figure 8, lower panel). No significant correlations were found at any frequency in the left hemisphere (O1 electrode). As previously demonstrated, USN patients showed 9 Hz SSVEP power in the

right hemisphere akin to healthy controls. However, right hemisphere responses correlated with symptom severity, which suggests a complex relationship between alpha-band SSVEP responses and spatial attention function in USN patients.

Discussion

We found that, even in the affected hemisphere, SSVEPs can be reliably elicited by flickering stimuli at various frequencies. This was expected because all of our stroke patients (i.e., both those with and without USN) had lesions in the right hemisphere but no hemianopsia. Notably, only the USN group exhibited a significant hemispheric difference in SSVEP at 9 Hz. In contrast to the healthy control group, this difference was attributed to an increase in activity within the intact hemisphere rather than a decrease in the affected hemisphere. Given the observation of increased PAC, we speculate that the enhanced response was due to better coordination between neural oscillations on the intact side. Furthermore, TE analysis revealed higher information flow from the visual cortex to the frontal cortex within the same hemisphere, which indicates an imbalance in information flow between hemispheres, in addition to local activity.

Alpha frequency-specific hemispheric bias and entrainment in USN patients

We observed hemispheric bias in entrainment to flickering stimuli in USN patients in the alpha band, which corresponds to the natural frequency of the visual system (Rosanova et al., 2009). The entrainment of the oscillatory system to an external stimulus is caused by the periodic phase shift of neural oscillations to the delivered pulse (Lakatos et al., 2019). At the EEG level, this is expressed as an increase in amplitude at the stimulus frequency as multiple oscillators begin to cycle in synchrony (Thut et al., 2011).

In general, entrainment is particularly effective when the stimulation period closely matches the oscillator's natural frequency (Pikovsky et al., 2003). This principle also applies to neural oscillations: rhythmic stimulation at frequencies that resonate with physiological rhythms influences cognitive and neural function by synchronizing task-related oscillations (Klimesch et al., 2003; Sauseng et al., 2009; Romei et al., 2011). Our previous research demonstrated that entrainment is most effective when the stimulation frequency closely matches the individual alpha frequency (Okazaki et al., 2021). We also observed that different brain regions have distinct natural frequencies, with entrainment being most pronounced in the alpha band in the visual cortex. Therefore, the observed bias in the 9-Hz frequency-specific SSVEP in USN

patients does not merely reflect a hemispheric difference in evoked visual responses to rhythmic external stimuli but, rather, a bias in the synchronous function of intrinsic neural oscillators in the visual area at a specific frequency band (i.e., the alpha band).

Local hemispheric bias of entrainment and attentional dysfunction in USN patients

Hyperactivity of the SSVEP and PAC in the left visual cortex in stroke patients may result from a lack of hemispheric reciprocal inhibition (Murase et al., 2004). This scenario is consistent with the concept that in USN, decreased inhibition from the affected right hemisphere causes overactivity of the visual cortex within the intact left hemisphere, which results in a left hemisphere bias in visual processing (Koch et al., 2008; Corbetta and Shulman, 2011). However, because this hemispheric bias was frequency-specific and was not observed in non-USN patients (who also had right hemisphere damage), it may reflect not only the overactivity of the visual cortex but also synchronization to external stimuli. The entrainment of neural oscillations to external stimuli is achieved via consistent phase alignment, which, in turn, systematically influences the timing of the higher frequency components of neural activity (Glim et al., 2019).

This coordination is influenced by both external factors and internal processes, such as attention in anticipatory contexts. Attention adjusts the temporal sequence of excitatory and inhibitory phases in neural oscillations, thereby influencing perception (Lakatos et al., 2008; Schroeder and Lakatos, 2009; Besle et al., 2011; Bonnefond and Jensen, 2012). Given the importance of alpha-band oscillations in attentional processes (Klimesch, 2012), the hemispheric bias in oscillatory synchrony observed in USN patients may reflect critical abnormalities in cortical excitability coordination. Therefore, the hemispheric bias in synchronization capacity at frequencies relevant to attention likely disrupts the coordinated oscillatory activity necessary for balanced spatial attention processing. This may contribute to the attentional deficits observed in patients with USN.

Biased information transfer in USN patients

Locally, the USN group showed a higher SSVEP and greater PAC in the left visual cortex, whereas TE from the right visual cortex to the left frontal cortex was higher than TE from the left visual cortex to the left frontal cortex. Given that right frontal damage is typical of patients with USN, this difference may be an adaptive neural response to maintain hemispheric communication and compensate for attentional

dysfunction. Specifically, input from the right visual cortex may bypass the affected right frontal cortex to enable enhanced information flow to the intact left frontal cortex, thereby supporting attentional functions. This compensatory strategy of increased information flow is consistent with functional imaging study findings on the reorganization of functional networks following stroke; moreover, it supports the idea of neuroplasticity, whereby patients can recover functions and maintain cognitive abilities following neurological injury (Nudo, 2006; Saur et al., 2006; Rehme et al., 2011).

Distinct neural responses in non-USN and USN patients

Although both the non-USN and USN groups had right hemisphere damage, they exhibited distinct neural responses to alpha-band rhythmic stimulation. In non-USN patients, additional neural resources were recruited from both hemispheres in response to the damage in the right hemisphere, resulting in enhanced neural synchronization to external stimuli across both hemispheres. In contrast, the neural responses in USN patients are more asymmetric, with a local increase in alpha-band SSVEP primarily observed in the intact left visual cortex. This asymmetry may result from the damaged right hemisphere being less effectively engaged, leading to an over-reliance on the left hemisphere (Corbetta et al., 2005). This suggests that the right hemisphere damage in USN patients might affect more critical parts of the attentional network.

Interestingly, even though we found no significant difference in right hemisphere alpha-band SSVEP power between the USN and healthy control groups, we observed a significant correlation between SSVEP power and BIT score. This suggests that although quantitative aspects, such as the amplitude of alpha-band oscillations in the right hemisphere, appeared normal, the involvement of these oscillations in spatial attention control networks from a qualitative perspective differs between USN patients and the healthy control and non-USN groups. Such qualitative differences in attentional processing may be reflected in BIT scores, abnormal responses in the intact (left) hemisphere, and changes in information transfer to frontal regions. However, the relationships among these elements may not necessarily be linear. Although our data cannot fully elucidate these complex interactions, our findings provide important insight into the role of alpha-band activity in USN.

Limitations

This study has several limitations that must be acknowledged. First, although we demonstrated a frequency-

specific hemispheric bias in patients with USN, the underlying neural mechanisms responsible for this bias remain unclear. Future studies using magnetoencephalography and other techniques with high spatiotemporal resolution would allow examinations of specific neural circuits. Second, we were unable to control for all potential confounders, particularly the precise extent and location of brain lesions in our patient groups. Although we matched patients according to stroke score, right hemisphere damage, and the absence of hemianopsia, differences in lesion characteristics (e.g., cortical vs. subcortical damage) may have influenced the results. Our frequency-specific findings suggest that our results are not solely attributed to general lesion effects. Nevertheless, future studies using larger sample sizes are needed to fully account for these variables. Third, the cross-sectional nature of this study limits our ability to draw definitive conclusions regarding causality. Longitudinal studies that track changes in neural oscillations and attentional performance over time would provide more insight into the causal relationships between neural synchrony and attentional deficits in USN patients.

Conclusions

Our study revealed critical differences in neural responses between USN patients and stroke patients without USN, particularly in the capacity to synchronize neural oscillations with external periodic inputs. In USN patients, we observed increased entraiment in the intact hemisphere, especially at the alpha frequency, whereas non-USN patients showed enhanced entrainment across both hemispheres. These distinct patterns suggest that certain features of right hemisphere damage in USN patients affect key components of the attention network, such as neural synchronization within the functionally important alpha frequency band. This frequency-specific alteration provides evidence for a unique pathophysiology of USN and its potential impact on spatial attention processes. Future research should explore these neural synchronization patterns in larger patient populations with USN and investigate their evolution during recovery and relationships with specific cognitive deficits. Furthermore, computational modeling studies of oscillatory network entrainment could offer insight into the mechanisms underlying the observed biases. Together, these strategies would provide a more comprehensive understanding of the complex neural dynamics involved in USN and how the altered synchronization patterns contribute to the unique pathophysiology of USN.

References

Besle J, Schevon CA, Mehta AD, Lakatos P, Goodman RR, McKhann GM, Emerson RG, Schroeder CE (2011) Tuning of the human neocortex to the temporal dynamics of attended events. J Neurosci 31:3176-3185.

Bonnefond M, Jensen O (2012) Alpha oscillations serve to protect working memory maintenance against anticipated distracters. Curr Biol 22:1969-1974.

Busch NA, Dubois J, VanRullen R (2009) The phase of ongoing EEG oscillations predicts visual perception. J Neurosci 29:7869-7876.

Castellanos NP, Makarov VA (2006) Recovering EEG brain signals: artifact suppression with wavelet enhanced independent component analysis. J Neurosci Methods 158:300-312.

Corbetta M, Shulman GL (2002) Control of goal-directed and stimulus-driven attention in the brain. Nat Rev Neurosci 3:201-215.

Corbetta M, Shulman GL (2011) Spatial neglect and attention networks. Annu Rev Neurosci 34:569-599.

Corbetta M, Kincade MJ, Lewis C, Snyder AZ, Sapir A (2005) Neural basis and recovery of spatial attention deficits in spatial neglect. Nat Neurosci 8:1603-1610.

Fiebelkorn IC, Saalmann YB, Kastner S (2013) Rhythmic sampling within and between objects despite sustained attention at a cued location. Curr Biol 23:2553-2558.

Fiebelkorn IC, Pinsk MA, Kastner S (2018) A Dynamic Interplay within the Frontoparietal Network Underlies Rhythmic Spatial Attention. Neuron 99:842-853 e848.

Glim S, Okazaki YO, Nakagawa Y, Mizuno Y, Hanakawa T, Kitajo K (2019) Phase-Amplitude Coupling of Neural Oscillations Can Be Effectively Probed with Concurrent TMS-EEG. Neural plasticity 2019:6263907.

Grefkes C, Fink GR (2011) Reorganization of cerebral networks after stroke: new insights from neuroimaging with connectivity approaches. Brain 134:1264-1276.

He BJ, Snyder AZ, Vincent JL, Epstein A, Shulman GL, Corbetta M (2007) Breakdown of functional connectivity in frontoparietal networks underlies behavioral deficits in spatial neglect. Neuron 53:905-918.

Karnath HO (2001) New insights into the functions of the superior temporal cortex. Nat Rev Neurosci 2:568-576.

Karnath HO, Ferber S, Himmelbach M (2001) Spatial awareness is a function of the temporal not the posterior parietal lobe. Nature 411:950-953.

Klimesch W (2012) alpha-band oscillations, attention, and controlled access to stored information. Trends Cogn Sci 16:606-617.

Klimesch W, Sauseng P, Gerloff C (2003) Enhancing cognitive performance with repetitive transcranial magnetic stimulation at human individual alpha frequency. Eur J Neurosci 17:1129-1133.

Koch G, Oliveri M, Cheeran B, Ruge D, Lo Gerfo E, Salerno S, Torriero S, Marconi B, Mori F, Driver J, Rothwell JC, Caltagirone C (2008) Hyperexcitability of parietal-motor functional connections in the intact left-hemisphere of patients with neglect. Brain 131:3147-3155.

Krishnan GP, Vohs JL, Hetrick WP, Carroll CA, Shekhar A, Bockbrader MA, O'Donnell BF (2005) Steady state visual evoked potential abnormalities in schizophrenia. Clin Neurophysiol 116:614-624.

Kwon JS, O'Donnell BF, Wallenstein GV, Greene RW, Hirayasu Y, Nestor PG, Hasselmo ME, Potts GF, Shenton ME, McCarley RW (1999) Gamma frequency-range abnormalities to auditory stimulation in schizophrenia. Arch Gen Psychiatry 56:1001-1005.

Lachaux JP, Rodriguez E, Van Quyen ML, Lutz A, Martinerie J, Varela FJ (2000) Studying single-trials of phase synchronous activity in the brain. Int J Bifurcat Chaos 10:2429-2439.

Lakatos P, Gross J, Thut G (2019) A New Unifying Account of the Roles of Neuronal Entrainment. Curr Biol 29:R890-R905.

Lakatos P, Karmos G, Mehta AD, Ulbert I, Schroeder CE (2008) Entrainment of neuronal oscillations as a mechanism of attentional selection. Science 320:110-113.

Legg PA, Rosin PL, Marshall D, Morgan JE (2013) Improving accuracy and efficiency of mutual information for multi-modal retinal image registration using adaptive probability density estimation. Comput Med Imaging Graph 37:597-606.

Maris E, Oostenveld R (2007) Nonparametric statistical testing of EEG- and MEG-data. J Neurosci Methods 164:177-190.

Mathewson KE, Gratton G, Fabiani M, Beck DM, Ro T (2009) To see or not to see: prestimulus alpha phase predicts visual awareness. J Neurosci 29:2725-2732.

Mathewson KE, Fabiani M, Gratton G, Beck DM, Lleras A (2010) Rescuing stimuli from invisibility: Inducing a momentary release from visual masking with pre-target entrainment. Cognition 115:186-191.

Mort DJ, Malhotra P, Mannan SK, Rorden C, Pambakian A, Kennard C, Husain M (2003) The anatomy of visual neglect. Brain 126:1986-1997.

Murase N, Duque J, Mazzocchio R, Cohen LG (2004) Influence of interhemispheric interactions on motor function in chronic stroke. Ann Neurol 55:400-409.

Notbohm A, Kurths J, Herrmann CS (2016) Modification of Brain Oscillations via Rhythmic Light Stimulation Provides Evidence for Entrainment but Not for Superposition of Event-Related Responses. Front Hum Neurosci 10:10.

Nudo RJ (2006) Mechanisms for recovery of motor function following cortical damage. Curr Opin Neurobiol 16:638-644.

Okazaki YO, Nakagawa Y, Mizuno Y, Hanakawa T, Kitajo K (2021) Frequency- and Area-Specific Phase Entrainment of Intrinsic Cortical Oscillations by Repetitive Transcranial Magnetic Stimulation. Front Hum Neurosci 15:608947.

Pikovsky A, Rosenblum M, Kurths J (2003) Synchronization - A Universal Concept in Nonlinear Sciences. Cambidge University Press.

Rehme AK, Fink GR, von Cramon DY, Grefkes C (2011) The role of the contralesional motor cortex for motor recovery in the early days after stroke assessed with longitudinal FMRI. Cereb Cortex 21:756-768.

Rojas DC, Teale PD, Maharajh K, Kronberg E, Youngpeter K, Wilson LB, Wallace A, Hepburn S (2011) Transient and steady-state auditory gamma-band responses in first-degree relatives of people with autism spectrum disorder. Mol Autism 2:11.

Romei V, Driver J, Schyns PG, Thut G (2011) Rhythmic TMS over parietal cortex links distinct brain frequencies to global versus local visual processing. Curr Biol 21:334-337.

Rosanova M, Casali A, Bellina V, Resta F, Mariotti M, Massimini M (2009) Natural frequencies of human corticothalamic circuits. J Neurosci 29:7679-7685.

Saur D, Lange R, Baumgaertner A, Schraknepper V, Willmes K, Rijntjes M, Weiller C (2006) Dynamics of language reorganization after stroke. Brain 129:1371-1384.

Sauseng P, Klimesch W, Heise KF, Gruber WR, Holz E, Karim AA, Glennon M, Gerloff C, Birbaumer N, Hummel FC (2009) Brain oscillatory substrates of visual short-term memory capacity. Curr Biol 19:1846-1852.

Schreiber T (2000) Measuring information transfer. Phys Rev Lett 85:461-464.

Schroeder CE, Lakatos P (2009) Low-frequency neuronal oscillations as instruments of sensory selection. Trends Neurosci 32:9-18.

Thiebaut de Schotten M, Urbanski M, Duffau H, Volle E, Levy R, Dubois B, Bartolomeo P (2005) Direct evidence for a parietal-frontal pathway subserving spatial awareness in humans. Science 309:2226-2228.

Thut G, Schyns PG, Gross J (2011) Entrainment of perceptually relevant brain oscillations by non-invasive rhythmic stimulation of the human brain. Front Psychol 2:170.

Tort AB, Komorowski R, Eichenbaum H, Kopell N (2010) Measuring phase-amplitude coupling between neuronal oscillations of different frequencies. J Neurophysiol 104:1195-1210.

Wilson TW, Rojas DC, Reite ML, Teale PD, Rogers SJ (2007) Children and adolescents with autism exhibit reduced MEG steady-state gamma responses. Biol Psychiatry 62:192-197.

Table 1. Demographic information of each group and clinical scores of the USN and non-USN patients matched by Mahalanobis distance

Variables	Mean ± SD			*p*-value (*U*-test)
	Non-USN	USN	Healthy control	
Number of participants	21	21 (16)	17	—
Sex	Male	Male	Male	—
Age (years)	68.4 ± 12.0	64.7 ± 14.0	63.0 ± 12.2	0.21, 0.91 (USN vs. non-USN, Healthy controls)
Cortical/subcortical lesion side	Right	Right	—	—
EEG recording (days poststroke)	33.2 ± 12.3	38.0 ± 12.0	—	0.19
FMA-UE (0–66)	37.3 ± 24.4	37.1 ± 23.8	—	0.93
FMA-LE (0–34)	22.4 ± 8.0	23.2 ± 8.7	—	0.92
FIM-M (13–91)	52.9 ± 19.0	49.4 ± 21.4	—	0.23
FIM-C (5–35)	27.2 ± 5.8	25.5 ± 8.0	—	0.13
BIT (0–222)	—	202.8 ± 17.3	—	—

Figure Legends

Figure 1. Experimental paradigm. The strobe light flickered for 10 s in 3-Hz steps from 3 Hz to 30 Hz with 10-s inter-train intervals. Participants were lying down with their eyes closed during the experiment.

Figure 2. SSVEP power for different response and flicker frequencies. Normalized power spectrum of the response frequency (y-axis) at the O2 electrode (affected hemisphere for patients) as a function of flicker frequency (x-axis). The fundamental frequency and the first harmonics (gray dashed lines) can be seen in all groups.

Figure 3. Hemispheric differences in SSVEP power at different flicker frequencies. Power in the intact hemisphere was stronger than that in the affected hemisphere with 9-Hz stimulation (***$p < 0.001$) in the USN group only (middle panel). Error bars represent 2 standard errors.

Figure 4. Hemispheric differences in SSVEP power at different flicker frequencies. There was no hemispheric difference between C3 and C4 electrodes (upper panels) and between F3 and F4 electrodes (lower panels) in any group. Error bars represent 2 standard errors.

Figure 5. SSVEP power during stimulation at 9 Hz and rest. Box plots indicate the power of SSVEP responses in the intact (O1 electrode) and affected (O2 electrode) hemispheres (left panels). A significantly higher response power was observed in the intact hemisphere of the USN group than in the left hemisphere of the healthy control group. The non-USN patients also displayed higher alpha power in both hemispheres than healthy controls without hemispheric bias (***$p < 0.001$). During the resting state interval (right panels), no significant differences in alpha power were observed between the USN and non-USN groups. Box plots depict medians and 25th/75th percentiles, with whiskers showing the 10th/90th percentiles overlaid onto individual data points (circles). The + represents outliers.

Figure 6. Hemispheric differences in PAC in response to 9-Hz flickering stimuli. The MI measuring the coupling between the alpha phase (7–12 Hz) and gamma power (35–45 Hz) represents the hemispheric

asymmetry in the USN group (indicated by the black outline). No such pattern was present in the non-USN or healthy control group.

Figure 7. Hemispheric differences in information flow between the visual and frontal areas in response to 9-Hz flickering stimuli. Box plots represent the differences in TE between the left and right hemispheres in the feedforward (upper panels) and feedback (lower panels) directions. The arrows on the topographical plots signify the direction of the TE comparison illustrated in the corresponding box plots. In the USN group, a significant hemispheric difference was observed in the feedforward direction (*$p < 0.05$), where the TE from the O2 electrode (right visual cortex) to the left frontal area was greater than the TE from the O1 electrode (left visual cortex) to the left frontal area. Moreover, this difference was significantly greater than that in the healthy control group (**$p < 0.01$). No significant hemispheric differences were observed in the feedforward direction in the non-USN or healthy control group or in the feedback direction in any of the groups. Box plots depict medians and 25th/75th percentiles, with whiskers showing the 10th/90th percentiles. The + represents outliers.

Figure 8. Correlation between SSVEP power and BIT score in USN patients. Scatter plots represent the relationship between SSVEP power at 9 Hz and BIT score for the left hemisphere (O1 electrode) and right hemisphere (O2 electrode; upper panels). A significant positive correlation was found in the right hemisphere ($r = 0.70$, $p < 0.01$) but not in the left hemisphere ($r = 0.38$, $p = 0.18$). The lower panel depicts the correlation coefficients between SSVEP power and BIT score across frequencies (3–30 Hz) for each hemisphere. Significant correlations were observed in the right hemisphere only at 9 and 12 Hz after FDR correction (**$p < 0.01$).

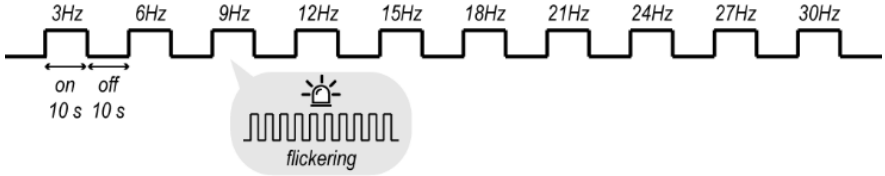
3Hz
6Hz
9Hz
12Hz
15Hz
18Hz
21Hz
24Hz
27Hz
30Hz
on
10 s
off
10 s
flickering

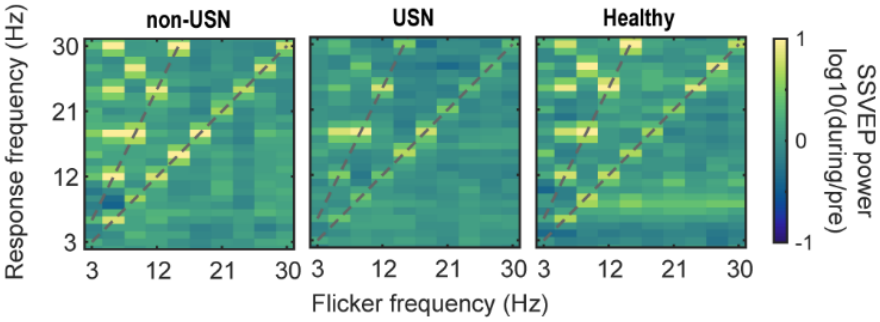
non-USN
USN
Healthy
Response frequency (Hz)
30
21
12
3
3
12
21
30
Flicker frequency (Hz)
1
0
-1
SSVEP power
log10(during/pre)

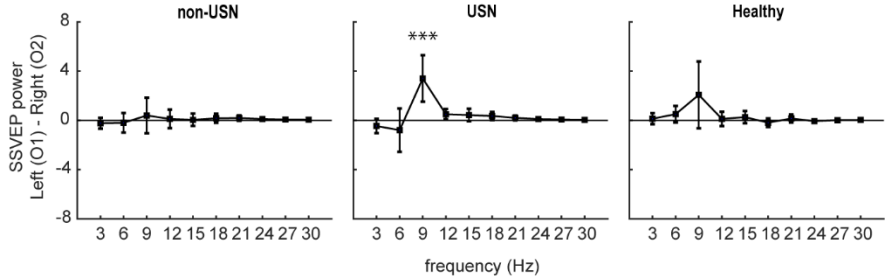
non-USN
USN
Healthy
***
SSVEP power
Left (O1) - Right (O2)
8
4
0
-4
-8
3 6 9 12 15 18 21 24 27 30
frequency (Hz)

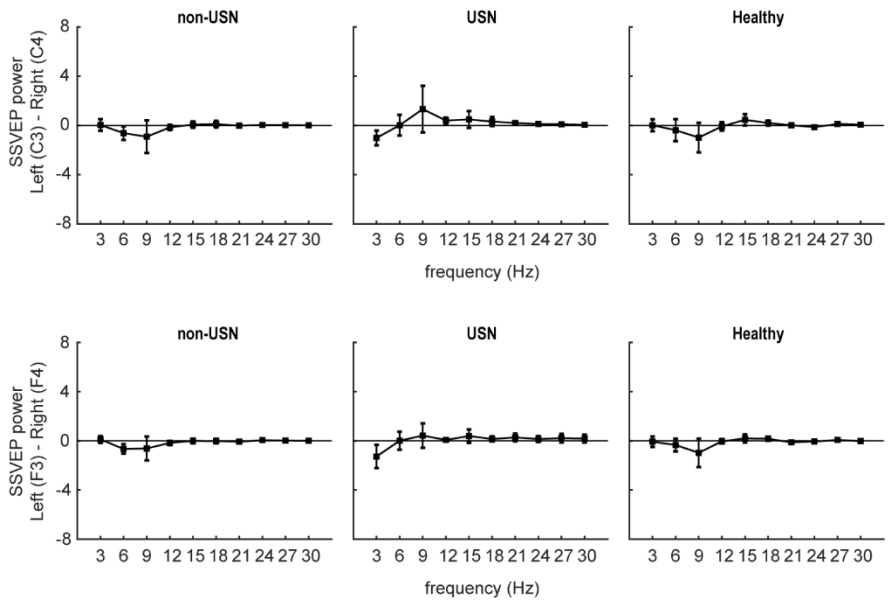
non-USN
USN
Healthy
SSVEP power
Left (C3) - Right (C4)
8
4
0
-4
-8
3 6 9 12 15 18 21 24 27 30
frequency (Hz)
non-USN
USN
Healthy
SSVEP power
Left (F3) - Right (F4)
8
4
0
-4
-8
3 6 9 12 15 18 21 24 27 30
frequency (Hz)

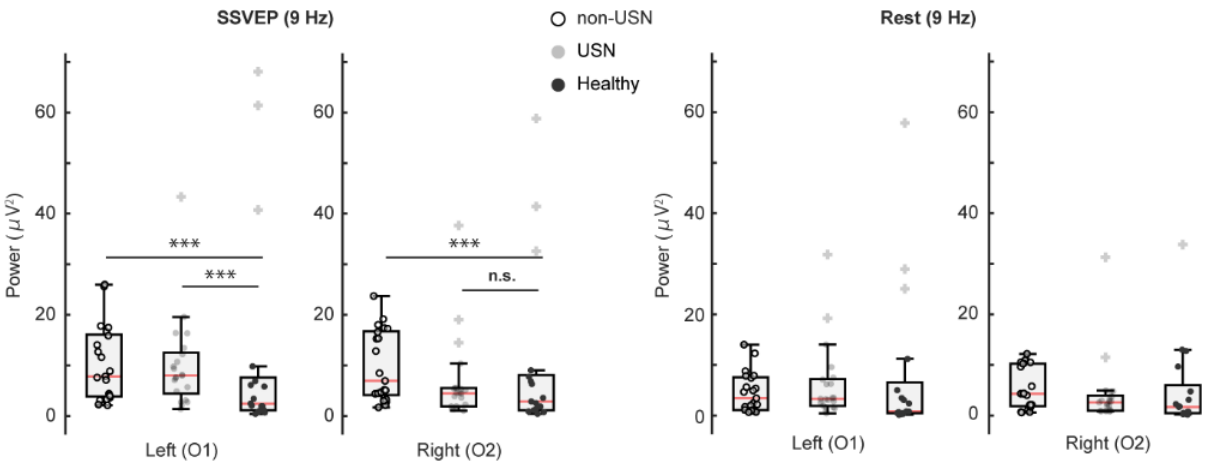
SSVEP (9 Hz)
non-USN
USN
Healthy
Rest (9 Hz)
Power (μV^2)
60
40
20
0
***
***
n.s.
Left (O1)
Right (O2)

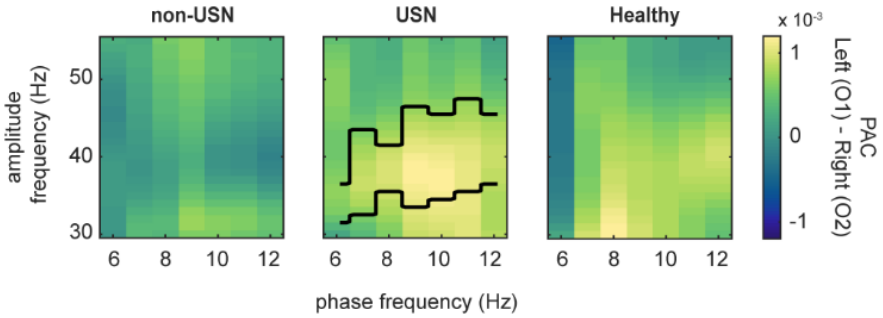
non-USN
USN
Healthy
amplitude frequency (Hz)
50
40
30
6
8
10
12
phase frequency (Hz)
x 10-3
1
0
-1
PAC
Left (O1) - Right (O2)

578

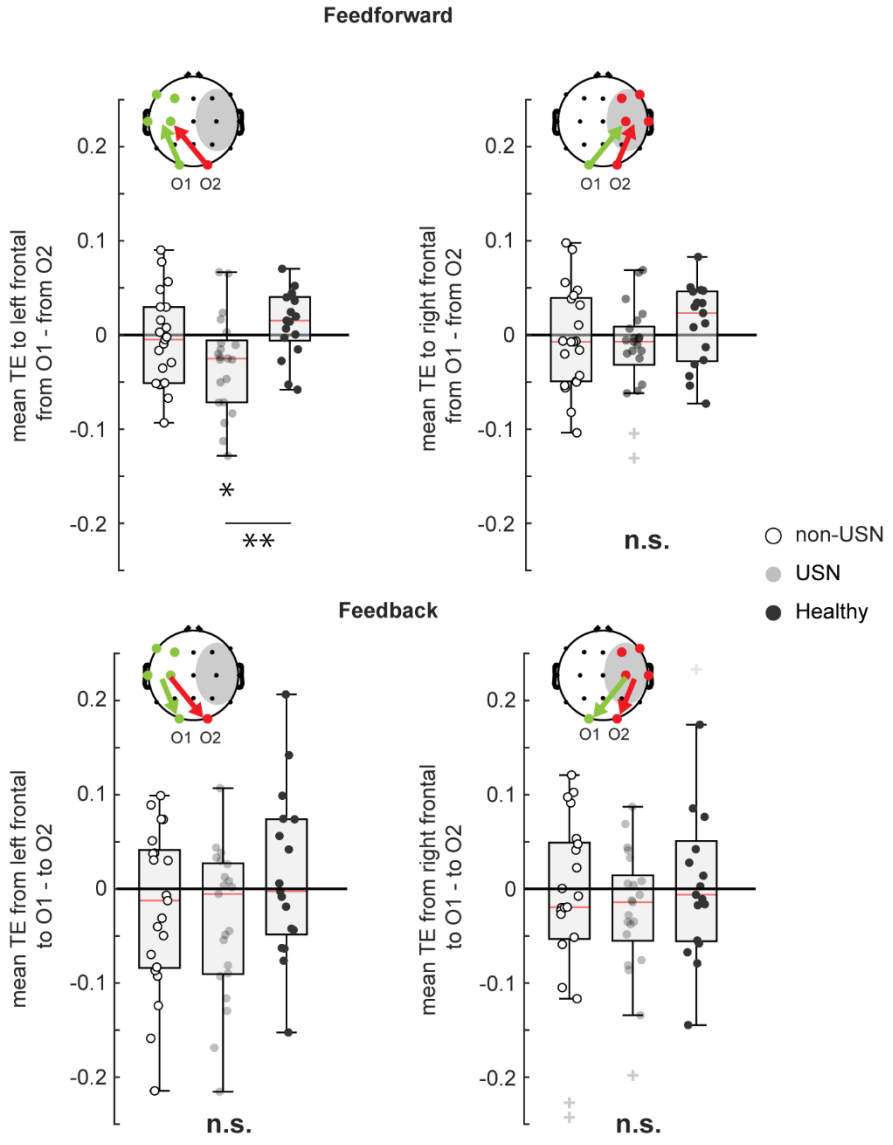
Feedforward
O1 O2
mean TE to left frontal from O1 - from O2
mean TE to right frontal from O1 - from O2
0.2
0.1
0
-0.1
-0.2
*
**
n.s.
non-USN
USN
Healthy
Feedback
mean TE from left frontal to O1 - to O2
mean TE from right frontal to O1 - to O2
n.s.
n.s.

579

580

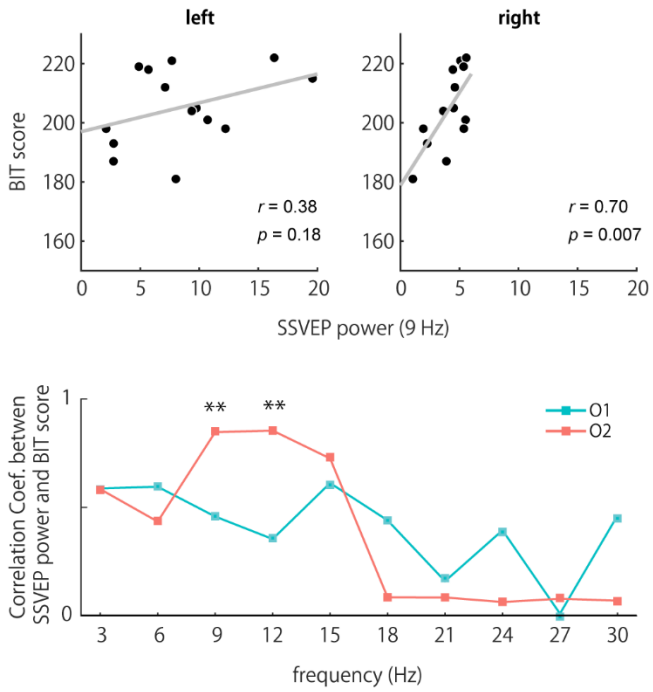
left
right
BIT score
220
200
180
160
0
5
10
15
20
r = 0.38
p = 0.18
r = 0.70
p = 0.007
SSVEP power (9 Hz)
Correlation Coef. betwen SSVEP power and BIT score
1
0
**
**
O1
O2
3
6
9
12
15
18
21
24
27
30
frequency (Hz)

581